

Coherent Pre-Distortion of Low-Frequency PLC Carriers

Stan McClellan
 Ingram School of Engineering
 Texas State University
 San Marcos, TX USA
 stan.mcclellan@txstate.edu

Michael L. Casey
 Ingram School of Engineering
 Texas State University
 San Marcos, TX USA
 mlcasey@txstate.edu

Matthias Chung
 Dept. of Mathematics
 Virginia Tech
 Blacksburg, VA USA
 mcchung@vt.edu

Abstract—The use of power lines for communication is a topic of great practical interest as well as active research and standardization activities. The introduction of communications signals onto an energized power line can cause significant distortion of the signal, especially at low frequencies. This paper describes a form of coherent pre-distortion for such communication signals which reduces the destructive interference. The approach can be optimized in several ways to mitigate distortion and achieve more efficient data transfer, and may be important in cases where low-frequency, low-rate carriers are used.

Keywords-Power line communications; PLC; pre-distortion;

I. INTRODUCTION

Transmission of data via an active power line is a difficult task, particularly at carrier frequencies below 2kHz [1]. As a result, the majority of activity in Power Line Communications (PLC) for Smart Grid applications has been in higher frequency bands [2]. At Very Low Frequencies (VLF), the pre-existing power signal on the line (the 50Hz or 60Hz “fundamental”) causes a number of problems in the system, including pseudo-stationary interference from harmonics of the fundamental and a form of “blowback” into the data transmitter. However, data communications at low frequencies can be very useful in a number of applications, such as Automatic Meter Reading (AMR), Advanced Metering Infrastructure (AMI) and similar command/control and data retrieval scenarios [1], [3].

Curiously, the structure of the power line network seems to interact in a specific fashion with low-frequency communication signals. This interaction can appear as a form of amplitude modulation of the communication signal, where the modulation envelope is phase-coherent or time-synchronous with the fundamental. An example of this phenomenon is shown in the top plot of Fig. 3. When present, this distortion envelope seems to be imposed on any/all secondary, low-frequency signals in the channel. We have not found any reference to this phenomenon in the literature. This type of channel-induced distortion is problematic for data communications because amplitude modulation creates harmonically-related images of the carrier frequency. As image signals proliferate, the availability of idle or useable spectrum for

additional subcarriers is reduced, and the dynamic placement of subcarriers becomes difficult.

An approach to counteracting such effects is to pre-distort the communication signal prior to introducing it into the channel. In this fashion, the distortion and pre-distortion effectively cancel each other out. The concept of pre-distortion is not new. For example, pre-distortion is often used to counteract nonlinearities in power amplifiers for wireless communications [4]–[6]. However, in the case of VLF PLC, nonlinearities seem to be introduced by the *channel itself*, which is a multi-port, multi-user network with time-varying characteristics, and so is very difficult to characterize completely. Pre-distortion techniques are also particularly important in channels with several subcarriers, or in systems using dynamic spectral allocation [7]–[10]. In the case of VLF PLC without effective pre-distortion, a multi-carrier PLC transmitter may be *prevented* from introducing additional subcarriers because the image signals from each subcarrier interfere very significantly with neighboring spectral bands. Furthermore, VLF PLC transmissions are very bursty and have very low data rates, making conventional equalization or filter-based pre-distortion difficult. Thus, we require a pre-distortion system which has a relatively simple formulation, is instantaneously applicable (no convergence delays), and effectively mediates spectral imaging due to channel effects.

This paper describes a specific approach to pre-distortion of a communication signal prior to introducing it onto an active power line in a VLF PLC system. The specific structure of the pre-distorted signal is important because it must be estimated very quickly from some functions of the signals on the channel. In our experimentation with VLF PLC on a live testbed, we have observed that for particular types of signals, the channel-induced distortion is synchronous with the fundamental. Refer to the top plot in Fig. 3 for an example of this phenomenon. Thus, we derive the form of the pre-distortion envelope from a model which is a linear combination of powers of the fundamental. Using this approach, the pre-distortion function can be computed instantaneously from observed samples of the fundamental. Thus, the method observes the extant voltage on the power network and, using the model of the distortion envelope, computes a pre-distortion function which can be imposed

on the communication signal just prior to introduction to the power network. In this fashion, we achieve a pre-distortion envelope which is a very close approximation to the amplitude distortion envelope imposed by the power network, and synchronous distortion is significantly reduced.

The remainder of this paper presents the approach to pre-distortion, including some motivating factors as well as experimental results exploring optimization of model parameters. Section II presents the mathematical formulation of the proposed channel model and pre-distortion function. The structure of the model is motivated using important considerations such as simplicity of form, ease of optimization, and synchronization with the fundamental. Section III presents experimental results using various configurations of the model to suppress channel-induced distortion. The effect of model order is explored using unit-valued coefficients, and the effect of coefficient optimization is discussed. Section IV concludes the paper by proposing extensions of the work to algorithmic optimization and implementation in a real-time system. The data used to develop this predistortion technique was gathered from an experimental powerline communication system which is being implemented on a production distribution grid. Simulations were developed to model the channel effects based on the acquired data, and were tested on a non-real-time PLC system. Implementation and optimization of the pre-distortion technique in a real-time, multi-carrier PLC system is ongoing.

II. MATHEMATICAL FORMULATION

The mathematical formulation of the pre-distorted signal and the method by which it is derived from observations of the fundamental are important factors in understanding the technique. In effect, the process creates a set of basis functions from an observation of the fundamental. These basis functions are combined and used to calculate the pre-distortion envelope, which is then applied to the communication signal. If the set of basis functions and their combination are a reasonable model of the unknown process creating amplitude distortion in the channel, then the two effects will counteract each other, leaving the communication signal in the channel undistorted. So, we propose a model based on a linear combination of functions of the power signal, and we show via simulation and deployment on a live testbed that this model effectively suppresses particular types of channel-induced distortion in VLF PLC.

Let $p(t)$, or simply p , be a power signal in the time domain with Fourier Transform $P(\xi) = \mathcal{F}(p)$. In a perfect channel, p would be simply a sinusoidal power signal with frequency 50Hz or 60Hz (the fundamental). In a realistic channel, p is the entire signal observed, which is largely sinusoidal but may contain some harmonic content, noise, etc. Much of the nonsinusoidal content is due to the electrical structure of the channel and the fundamental excitation.

Let $x(t)$, or x , be a communication signal in the time domain with Fourier Transform $X(\xi) = \mathcal{F}(x)$. In the simplest case, x might be a sinusoid at some frequency other than 50Hz or 60Hz. In other cases, x might be a more complex passband carrier, modulated via analog or digital means to carry a message signal or data bits.

The objective is to transmit communication signal x through the power line system so that the resulting signal can be recovered by the receiver without error. Unfortunately, during transmission the power line system distorts x via an unknown transfer function $H_p(x)$. Due to the nature of the system, the transfer function does not affect the power signal p . In fact, the transfer function H_p seems to depend on p in some fashion, and although H_p cannot be observed directly, the structure of H_p can be partially estimated via observation of p . Since the effect of H_p is similar to conventional amplitude modulation, appropriate pre-distortion of x via an inverse-function H_p^{-1} will approximately account for the channel's envelope distortion, thereby suppressing any unwanted noise or spectral artifacts which are related to the interaction of x , p , and H_p . Mathematically,

$$H_p(H_p^{-1}(x)) = x. \quad (1)$$

Computing H_p^{-1} precisely is impossible. Fortunately, we can estimate the structure of H_p using powers of the fundamental p . This produces the approximation \hat{H}_p^{-1} and the pre-distorted signal $y = \hat{H}_p^{-1}(x)$ so that (1) becomes

$$H_p(y) = \hat{x} \approx x. \quad (2)$$

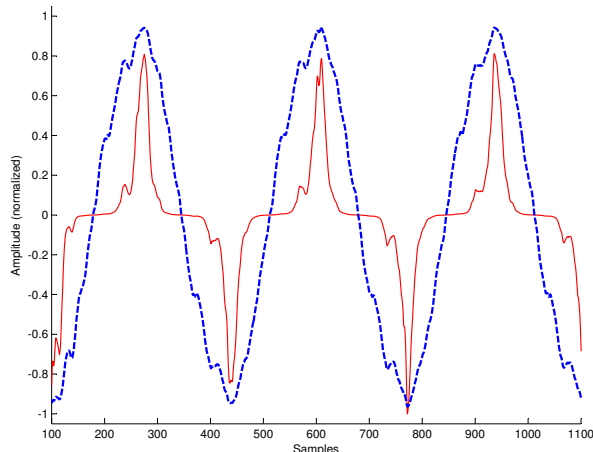
By choosing the structure of \hat{H}_p^{-1} carefully (the model), any errors in the approximation of H_p can be reduced significantly via one of several well-known methods [11]–[13].

A. Modeling H_p

Although H_p is difficult to model, we have observed that the channel produces a coherent amplitude modulation of secondary signals such as x . Refer to the top plot of Fig. 3 for an example of this phenomenon. By analyzing data acquired from an experimental PLC system which evidences this behavior, the authors have discovered that the channel-induced modulation can be partially modeled using a linear combination of powers of p , or

$$q(t, \alpha) = \sum_{j=1}^N \alpha_j [p(t)]^j, \quad (3)$$

where coefficients $\alpha = (\alpha_1, \dots, \alpha_N)^\top$ are initially unknown and must be optimized for each instance of the channel or re-optimized over time. A representative p and q are shown in Fig. 1 where the coefficients α have been estimated manually, p and q are normalized to unit amplitude, and q is formulated using only odd powers of p (i.e. $\alpha_j = 0$ for j even).


 Figure 1. p (dashed line) and q (solid line).

Using terms familiar to communications systems, the channel constructs a “false message” which is imposed on communication signal x as it transits the channel. Here, we use the unknown transfer function H_p to represent the false message signal. Estimating H_p via q provides an easily-constructed relationship given by:

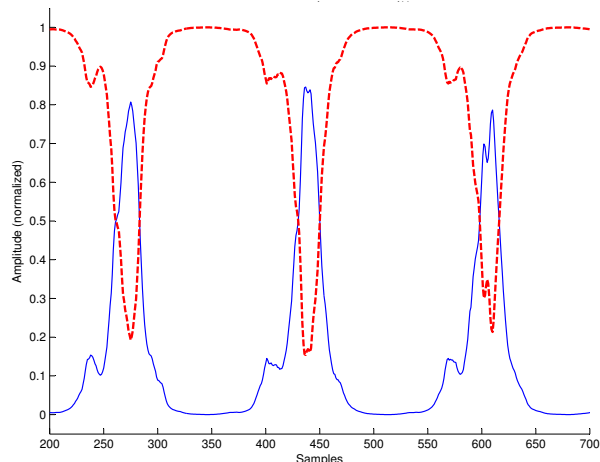
$$\hat{H}_p(t, \alpha) = -|q(t)| + \delta. \quad (4)$$

In (4), the false message H_p is estimated by \hat{H}_p , which depends on q through coefficients α . The false message can be counteracted by pre-distorting x with \hat{H}_p^{-1} . As in typical modulation practices, all envelope functions are normalized to unit amplitude prior to use. In (4), δ is a constant related to the modulation depth, as is customary for amplitude modulation envelopes [14]. A representative modulation envelope H_p recovered from an actual power signal is shown in Fig. 2, along with the estimated inverse envelope \hat{H}_p^{-1} . In the figure, the signals are shown normalized to unit amplitude, and have not been scaled for correct modulation depth, i.e. $\delta = 0$.

A representative distorted signal $H_p(x)$ is shown in the top plot of Fig. 3. In this case, x is a sinusoid with frequency of roughly 900Hz. Note the subtle amplitude modulation effects of H_p on x . The amplitude envelope of the modulated signal has periodic notches which are synchronized with the peaks of p . These time-domain attributes are implicitly modeled very accurately and simply by q and hence \hat{H}_p . Thus, the envelope can easily be translated to an optimized pre-distortion implementation \hat{H}_p^{-1} which does not require complex feedback loops or phase discrimination/locking techniques.

B. Coherent pre-distortion

To achieve effective communication, the modulation imposed by the channel via H_p must be pre-distorted by an inverse function. The pre-distortion approach involves


 Figure 2. Estimated channel modulation envelope H_p (dashed line) and corresponding pre-distortion envelope \hat{H}_p^{-1} (solid line). Both signals are normalized to unit amplitude, and are shown prior to scaling for appropriate modulation depth.

estimating and optimizing the coefficients of q and then formulating an estimated false message signal \hat{H}_p which can be applied to x prior to introduction to the channel via \hat{H}_p^{-1} . Upon introduction to the channel, the channel transfer function re-imposes the false message H_p onto the pre-distorted signal. In this fashion, the distortion due to the channel can be modeled as in (2), subject to the fidelity of α , q , and hence \hat{H}_p . The outcome of this process is shown in Fig. 3, which displays plots of the channel signal $H_p(x)$, the pre-distorted signal y , and the resulting suppressed signal $\hat{x} \approx x$. For the figure, the communication signal x (not shown) was a low-rate BPSK-modulated carrier at approximately 900Hz, and the resultant signals are shown offset for clarity and normalized to approximately unit amplitude.

The optimization of the pre-distortion envelope \hat{H}_p^{-1} and the coefficients α so that $\hat{x} \approx x$ is an extremely complex problem, and the subject of further study. Clearly, when \hat{H}_p equals H_p exactly, the communication signal x will transit the channel undistorted by coherent amplitude modulation. Unfortunately, as mentioned previously, the form of H_p is unknown, and must be modeled via q , so that determining an envelope function $\hat{H}_p \approx H_p$ is not trivial.

The pre-distortion envelope \hat{H}_p^{-1} will be used in a conventional double-sideband amplitude modulation (DSB-AM) [14], and so must be normalized to unit amplitude before use. Thus, a formulaic representation of \hat{H}_p^{-1} is:

$$\hat{H}_p^{-1}(t, \alpha) = \frac{|q(t)| + \varepsilon}{c}, \quad (5)$$

where $\alpha = (\alpha_1, \dots, \alpha_N)^\top$, $\varepsilon > 0$, and $c = \max\{|q(t)| + \varepsilon\}$ to ensure unit amplitude. A representative envelope is shown in Fig. 2 (solid line), and the effect of applying the envelope to a communication signal x is shown in Fig. 3 (middle plot).

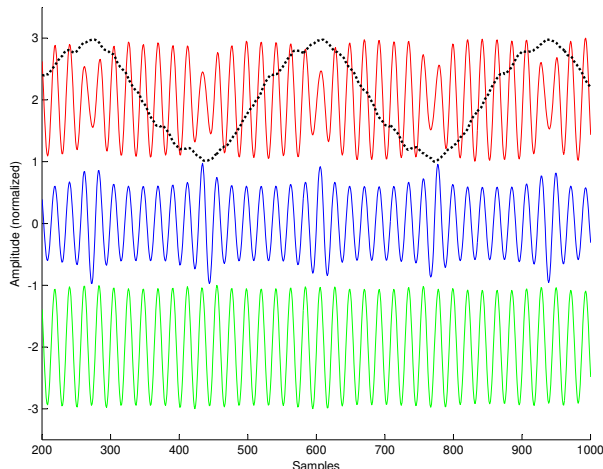


Figure 3. Top: distorted signal $H_p(x)$ and power signal $p(t)$ (dotted line); Middle: pre-distorted signal y ; Bottom: resulting signal \hat{x} , which approximates x . All signals are normalized to unit amplitude, and have been offset for clear display.

In Fig. 3 the coefficients α have been estimated manually. However even with non-optimal coefficients, the fidelity of the pre-distortion process leads to accurate reconstruction of the signal x , as can be seen from the bottom plot in Fig. 3 (\hat{x}) and the spectral plot in Fig. 5.

Estimation and inversion of the false message reduces to an optimization problem which depends on a linear combination of basis functions and the set of coefficients α . A number of well-known methods exist for optimizing coefficients of this form, such as Least Mean Squares (LMS), Recursive Least Squares (RLS), etc. [15], [16]. However, optimization of the coefficients α leads to a non-smooth optimization problem which needs to be targeted either by direct search methods [11] or by gradient-based optimization methods after a smoothing process. Note that the signal p is changing slowly over time, so the introduction of a windowed or framed approach is likely optimal, but forward-adaptive or backward-adaptive methods for re-optimizing α are subjects of further study.

III. RESULTS USING NON-OPTIMIZED PARAMETERS

The optimal form of the pre-distortion problem is important, but is also very difficult and the subject of considerable research effort by the authors using both simulations and testing on an experimental PLC system. However, even in the absence of complete optimization we can demonstrate the utility of the proposed model using *manually optimized* parameters. In the case of manual optimization, there are two primary dimensions in (3) that must be considered: (a) the values of α , and (b) the order of the model, N . Following subsections describe evaluation of the parameters of (3) and the overall predistortion process via model order and coefficient selection.

A. Effect of Model Order

Important optimizations for the pre-distortion system are the selection of “best” model order (N) and resulting coefficient structure. We have noticed via both simulation and experimentation in a live PLC system that the effect of odd-powers and even-powers of p in (3) and the pre-distortion envelope in (5) is pronounced and important. Thus, we briefly examine the effects of model order and coefficient structure in the formulation of q . To evaluate the noted effects, we simulate the pre-distortion system using model configurations with unit-valued coefficients and odd-only or even-only powers of p and model orders $N < 100$. Using this simulation, we compute the usual zero-mean signal-to-noise ratio (SNR) between the compensated signal \hat{x} and the original signal x according to (6), where $x[n]$ denotes the discrete-time (sampled) signal x .

$$\text{SNR (dB)} = 10 \log_{10} \left(\frac{\sum x[n]^2}{\sum (x[n] - \hat{x}[n])^2} \right) \quad (6)$$

Fig. 4 summarizes the simulation results for distortion versus model structure using (3) and the resultant pre-distortion process. In the figure, the curve labeled “all coefficients” has $\alpha_j = 1 \forall j$, whereas the curve labeled “even coefficients” has $\alpha_j = 1$ for j even, and $\alpha_j = 0$ otherwise (similarly for “odd coefficients”). Note from the figure that although the combined odd/even model seems to result in reasonable distortion for lower model orders ($N < 10$), the effect of model order is very pronounced. So, for lower model orders and combined odd/even model construction, the system is extremely sensitive to variations in model order and input data. Conversely, for moderate model orders ($10 < N < 50$) both the odd-only and even-only model constructions perform better than the combined construction, and exhibit very little sensitivity to model order. Notably, for moderate model orders, the odd-only construction ((3) with $\alpha_j = 1$, j odd) reaches a *higher maximum* SNR, and evidences a *smoother ascent*. As a result, the process of optimizing odd-only coefficient vectors α may be less prone to local extrema. Additionally, for large model orders ($N > 50$), the differential distortion between odd-only, even-only, and odd-even model constructions is insignificant. From this result, we conclude that the use of odd-only powers of p in (3) produces harmonic suppression which is more effective for subbands which are more prevalent in the distortion characteristic of the channel.

B. Manual Optimization

Illustrative results for manually optimized coefficients α are shown in Fig. 3, where an approximately sinusoidal signal x with frequency around 900Hz is introduced to the channel. The figure uses data acquired from our VLF PLC testbed. In the figure, the effect of the coherent, channel induced distortion $H_p(x)$ is evident in the top plot, and the pre-distorted signal y in the middle plot is fed to the channel,

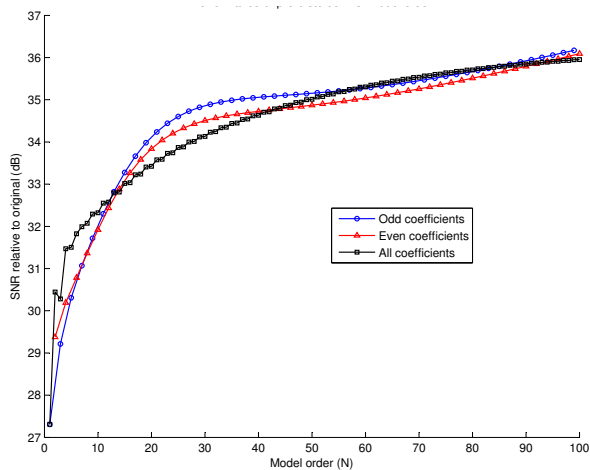


Figure 4. Distortion versus model order for odd-only, even-only, and odd/even model constructions with unit-valued coefficients.

resulting in the bottom plot where $\hat{x} \approx x$ and the distortion is suppressed.

In the top plot of Fig. 3, note the subtle modulation of the amplitude of x due to H_p . The periodic notches in the amplitude of $H_p(x)$ are synchronous with the peaks of p , which is shown overlaid on the top plot of Fig. 3 with unit amplitude. In the middle plot, note the corresponding inverse amplitude modulation of x due to \hat{H}_p^{-1} . The periodic peaks in the amplitude of y are aligned with the peaks of p , and hence are also aligned with the periodic notches in $H_p(x)$. These time-domain attributes are accurately modeled by q and hence y , which results in a straightforward pre-distortion approach. Thus, when the pre-distorted signal y is introduced to the channel, $H_p(y) = \hat{x} \approx x$ as in (2), and as shown in the bottom plot of Fig. 3.

The effect of this process becomes particularly clear in Fig. 5 which overlays spectra of the idle channel, the channel with distorted input, and the compensated signal \hat{x} , and the inset, which overlays spectra of the distortion before and after the pre-distortion process. In the figures, a low-rate BPSK signal x is introduced to the channel with a carrier frequency near 900Hz. When the pre-distortion scheme is not used, the images or sidelobes of the introduced signal are clearly evident in both figures at 120Hz harmonic offsets from the carrier (i.e. $900\text{Hz} \pm (n \times 120\text{Hz})$). However, when the pre-distortion scheme is used, the images of x are suppressed significantly. Also note the roughly 20dB suppression of the image signals nearest the 900Hz carrier (cf. 400-800Hz and 1000-1400Hz). In this case, the differential distortion between the original communication signal x and the pre-distorted signal \hat{x} is less than 0.5dB. Note also that imperfections due to non-optimal coefficients α results in two areas which need additional optimization: (a) spurious peaks at distant 120Hz harmonic offsets from the 900Hz carrier (cf. 1600-1800 and 100-200Hz), and (b) a slowly

varying spectral envelope. In these tests, we do not compare end-to-end performance metrics such as bit-error rate (BER) because the effect of the channel-induced distortion can easily be mitigated for single-carrier systems via the use of a high-quality receive filter. Instead, our VLF PLC system is targeted for multi-carrier architecture using dynamic channel selection, and the suppression of coherent images is a critical first-step in the implementation of that architecture.

IV. CONCLUSION

The suppression of image signals in low-frequency, narrowband PLC systems can be important. When optimized and deployed in a system which continuously re-optimizes the coefficients α , the near-field suppression approach described here may yield significant benefits for transmission schemes which rely on large numbers of low-rate carriers, such as frequency-division modulation (FDM) or computationally efficient equivalent approaches based on transforms, such as orthogonal FDM (OFDM).

The pre-distortion model proposed here has been shown to be efficiently realized and capable of instantaneous implementation with no requirements for phase-locking or delay due to convergence of an adaptive filter. These implementation details are extremely important in a VLF PLC system with bursty, low-rate transmissions. In initial testing of the approach using non-adaptive, hand-optimized coefficients, we have achieved greater than 20dB suppression of channel-induced distortion in critical subbands, making these areas of the spectrum available for dynamic allocation by the transmitter.

The authors are actively pursuing algorithmic optimizations of critical model parameters, including model order, coefficient selection, and adaptation rate for implementation in a real-time, low-frequency PLC communication system being implemented on a local distribution grid.

REFERENCES

- [1] D. Rieken, "Periodic noise in very low frequency power-line communications," in *IEEE Int. Symp. Power Line Comms and Appl. (ISPLC)*, Apr. 2011, pp. 295 – 300.
- [2] M. Nassar, J. Lin, Y. Mortazavi, A. Dabak, I. H. Kim, and B. L. Evans, "Local utility powerline communications in the 3-500 kHz band: Channel impairments, noise, and standards," *IEEE Sig. Proc. Mag. Special Issue on Sig. Proc. Techn. for the Smart Grid*, vol. 29, no. 5, pp. 116–127, Sep. 2012.
- [3] S. Galli, A. Scaglione, and Z. Wang, "Power line communications and the Smart Grid," in *IEEE Int. Conf. Smart Grid Comms (SmartGridComm)*, Oct. 2010, pp. 303 – 308.
- [4] Y. Y. Woo, J. Kim, J. Yi, S. Hong, I. Kim, and B. Kim, "Adaptive digital feedback predistortion technique for linearizing power amplifiers," *IEEE Trans. Microw. Theory Tech.*, vol. 55, no. 5, pp. 932–940, 2007.

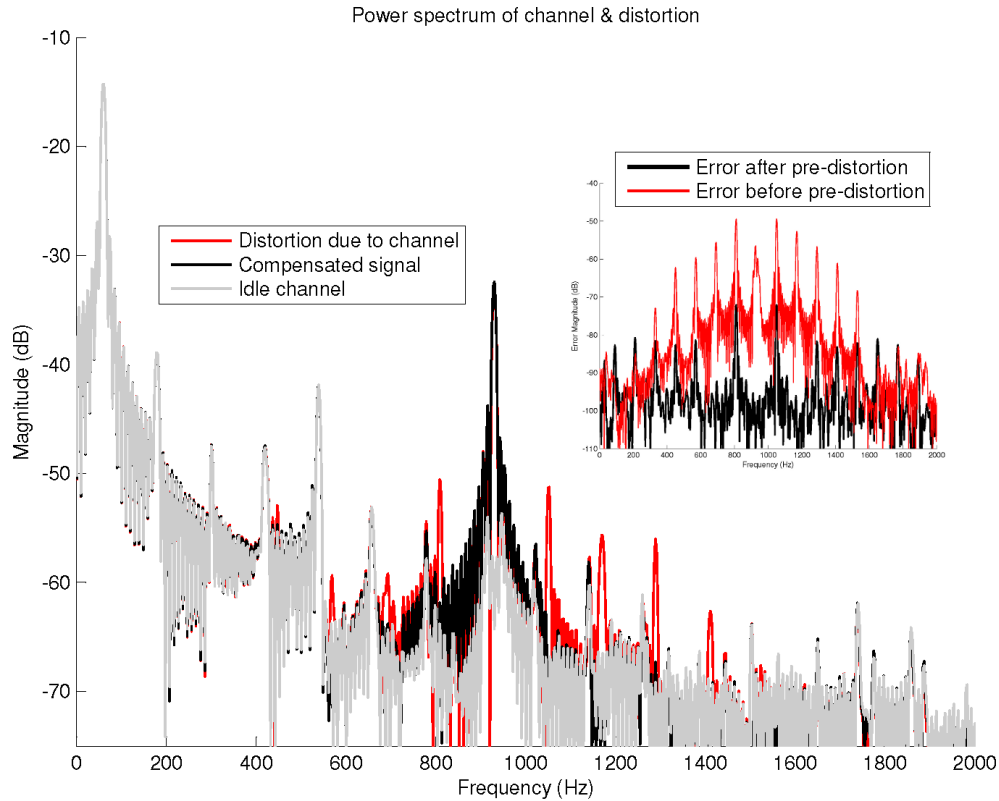


Figure 5. Power spectrum of channel before and after pre-distortion process via estimates of q and application of pre-distortion envelope \hat{H}_p^{-1} . The error signal spectra are shown in the inset. The spectrum of the compensated signal \hat{x} and the spectrum of the stimulus signal x are almost identical, and the channel-induced distortion is effectively suppressed.

- [5] S. Chung and J. L. Dawson, "Digital predistortion using quadrature $\Delta\Sigma$ modulation with fast adaptation for wlan power amplifiers," in *IEEE Microwave Symposium Digest (MTT)*, June 2011, pp. 1–4.
- [6] J. X. Qiu, D. K. Abe, T. M. Antonsen, B. G. Danly, B. Levush, and R. E. Myers, "Linearizability of TWTAs using predistortion techniques," *IEEE Trans. Electron Devices*, vol. 52, no. 5, pp. 718–727, 2005.
- [7] J. Shen, S. Liu, Y. Wang, G. Xie, H. Rashvand, and Y. Liu, "Robust energy detection in cognitive radio," *IET Communications*, vol. 3, no. 6, pp. 1016–1023, June 2009.
- [8] P. D. Sutton, K. Nolan, and L. Doyle, "Cyclostationary signatures in practical cognitive radio applications," *IEEE J. Sel. Areas Commun.*, vol. 26, no. 1, pp. 13–24, 2008.
- [9] B. Farhang-Boroujeny and R. Kempter, "Multicarrier communication techniques for spectrum sensing and communication in cognitive radios," *IEEE Commun. Mag.*, vol. 46, no. 4, pp. 80–85, Apr. 2008.
- [10] P. Pawelczak, K. Nolan, L. Doyle, S. W. Oh, and D. Cabric, "Cognitive radio: Ten years of experimentation and development," *IEEE Commun. Mag.*, vol. 49, no. 3, pp. 90–100, 2011.
- [11] J. Nelder and R. Mead, "A simplex method for function minimization," *Computer Journal*, vol. 7, pp. 308–313, 1965.
- [12] R. Fletcher, *Practical Methods of Optimization*. New York, NY: Wiley, 1987.
- [13] H. Matthies and G. Strang, "The solution of non linear finite element equations," *Int. J. Num. Methods in Engr.*, vol. 14, pp. 1613–1626, 1979.
- [14] J. M. Wozencraft and I. M. Jacobs, *Principles of Communication Engineering*. Prospect Heights, IL: Waveland Press, 1990.
- [15] S. Haykin, *Adaptive Filter Theory*. Prentice-Hall, 1986.
- [16] B. Widrow and S. Stearns, *Adaptive Signal Processing*. Prentice-Hall, 1985.